Journal of Alloys and Compounds 657 (2016) 537–545

Contents lists available at ScienceDirect

Journal of Alloys and Compounds

journal homepage: http://www.elsevier.com/locate/jalcom

Properties and electrochemical performance of $Sr_{0.8}La_{0.2}TiO_{3-\delta}$-$Ce_{0.8}Gd_{0.2}O_{2-\delta}$ composite anodes for intermediate temperature solid oxide fuel cells

Manasa K. Rath [a], Ki-Tae Lee [a, b, *]

[a] Division of Advanced Materials Engineering, Chonbuk National University, Jeonbuk, 561-756, Republic of Korea
[b] Hydrogen and Fuel Cell Research Center, Chonbuk National University, Jeonbuk, 561-756, Republic of Korea

ARTICLE INFO

Article history:
Received 17 August 2015
Received in revised form
8 October 2015
Accepted 19 October 2015
Available online 21 October 2015

Keywords:
Solid oxide fuel cell
Percolation
Composite anode
Polarization resistance

ABSTRACT

A series of $Sr_{0.8}La_{0.2}TiO_{3-\delta}$ (SLT)-$Ce_{0.8}Gd_{0.2}O_{2-\delta}$ (GDC) composite anodes with various volume ratios of SLT and GDC has been synthesized using a sucrose modified combustion technique. The percolation thresholds of $Sr_{0.8}La_{0.2}TiO_{3-\delta}$ and $Ce_{0.8}Gd_{0.2}O_{2-\delta}$ in the composite calculated based on the Kusy's percolation theory were 75.6 vol.% and 36.1 vol.%, respectively. While the rate of carbon deposition increased with an increase in the $Ce_{0.8}Gd_{0.2}O_{2-\delta}$ content, the total electrical conductivity decreased in humidified H_2 as well as in CH_4. Based on the electrochemical performance measured using AC-impedance spectroscopy, the optimal anode composition was 65 vol.% $Sr_{0.8}La_{0.2}TiO_{3-\delta}$-35 vol.% $Ce_{0.8}Gd_{0.2}O_{2-\delta}$. This composite has polarization resistances of 2.80 Ω cm^2 and 4.60 Ω cm^2 in H_2 and CH_4, respectively, measured at 800 °C. Diffusion or concentration polarization was the rate determining steps for the fuel oxidation process in the $Sr_{0.8}La_{0.2}TiO_{3-\delta}$-$Ce_{0.8}Gd_{0.2}O_{2-\delta}$ composite anode.

1. Introduction

The state-of-the-art nickel-yttria stabilized zirconia (Ni-YSZ) anodes used in solid oxide fuel cells (SOFCs) have superior catalytic properties for hydrogen oxidation, excellent chemical stability and compatibility with other cell components, and a very high electrical conductivity in a reducing atmosphere [1–3]. However, there are some serious limitations in these Ni-cermet anode systems including cell performance degradation during long-term operation, Ni coarsening, poor redox stability, and coking/deactivation of the Ni by fuel containing hydrocarbons and sulfur [4–8]. To address these issues, mixed ionic and electronic conducting (MIEC) materials with excellent electro-catalytic and electrochemical performance have been investigated. Perovskite-based oxide anodes can be operated in either fossil or biogas fuels that contain sulfur or higher hydrocarbon impurities. Among the numerous perovskite based anode materials, $SrTiO_3$- or $LaCrO_3$-based anodes have shown very high electrical conductivity as well as stability in reducing atmospheres [3,9,10].

$SrTiO_3$-based perovskite oxide doped with rare earth metal (Ce, Y, and La) on the A-site shows high catalytic activity, very high electrical conductivity, and high chemical stability compared to other perovskite-based anode materials [11–14]. In $SrTiO_3$, the Ti on the B site has two oxidation states (Ti^{3+} and Ti^{4+}). Ti^{4+} converts to a lower oxidation state under a reducing atmosphere, which effectively creates electronic charge carriers that facilitate the electrocatalytic processes and provide electronic conductivity. On the other hand, doping with high valence cations on the A-site leads to non-stoichiometric oxygen content under reducing conditions. This maintains overall charge neutrality, and the formation of oxide ion vacancies enhances the oxide ion conductivity of the materials. Therefore, cation doping of $SrTiO_3$ can be used to improve its catalytic activity and its mixed ionic and electronic conduction (MIEC) properties. Among the various rare earth doped $SrTiO_3$ materials, La-doped $SrTiO_3$ (SLT) has shown good chemical and dimensional stability over a wide range of temperatures and oxygen partial pressures [15–19]. Furthermore, the thermal expansion coefficient (TEC) of La-doped $SrTiO_3$ is similar to that of the $La_{0.8}Sr_{0.2}Ga_{0.8}Mg_{0.2}O_3$ (LSGM) electrolyte [16,20]. La-doped $SrTiO_3$ also shows good stability for fuels containing H_2S and shows high resistance to carbon coking when in the presence of hydrocarbon fuels [21–24]. However, the SLT still shows relatively worse

---

[*] Corresponding author. Division of Advanced Materials Engineering, Chonbuk National University, Jeonbuk, 561-756, Republic of Korea.
E-mail address: ktlee71@jbnu.ac.kr (K.-T. Lee).

http://dx.doi.org/10.1016/j.jallcom.2015.10.171
0925-8388/© 2015 Elsevier B.V. All rights reserved.

electrochemical performance compared to Ni-based anodes under humidified H_2. Hence, SLT is combined with other oxide ion conductors or active catalysts in order to improve the electrochemical performance [25].

Recently, many composite anodes of SLT have been reported, including SLT-YSZ, SLT-CeO_2, and Pd-SLT-CeO_2 [26–29]. The Gd-doped CeO_2 (GDC)-SLT based composite anode showed significantly enhanced performance in both humidified H_2 and CH_4 [23,30,31]. However, a systematic investigation of the factors that control the electro-catalytic activity of SLT-GDC composite anodes is not available in the literature. Therefore, we prepared $Sr_{0.8}La_{0.2}TiO_{3-\delta}$-$Ce_{0.8}Gd_{0.2}O_{2-\delta}$ (SLT-GDC) composites with various volume ratios in order to confirm the optimal composition, and we evaluated the electro-catalytic activity. We determined the effect of percolation on the microstructure, the electrical conductivity, the carbon deposition, and the electrochemical performance.

2. Experimental

2.1. Powder synthesis

SLT-GDC composites were synthesized by a modified sol–gel combustion technique using sucrose and pectin as fuel and as a catalyst, respectively. The starting materials used in this process were $La(NO_3)_3\cdot5H_2O$ (Aldrich, 99.9% metal basis), $Sr(NO_3)_2$ (Alfa Aesar, 99.0%), $(CH_3CH(O\text{-})NH_4)_2Ti(OH)_2$ (50%w/w aqueous solution, Alfa Aesar), $Gd(NO_3)_2\cdot6H_2O$ (Alfa Aesar, 99.9%, ACS), $Ce(NO_3)_2\cdot6H_2O$ (Alfa Aesar, 99.9%), sucrose (Alfa Aesar, 99%), and pectin (Aldrich). A flowchart for the combustion method is provided in Fig. 1. The synthesized compositions and their abbreviations are listed in Table 1.

2.2. Materials characterization

The synthesized composite anodes were characterized by X-ray diffraction (XRD) using Cu-Kα radiation for phase analysis. Diffraction patterns were recorded at a scan rate of 4° min^{-1} in a 2θ range from 20° to 80°. The XRD patterns were analyzed using the JADE software with powder diffraction files. We used scanning electron microscopy/energy-dispersive X-ray spectroscopy (SEM/EDX, SN-3000 Hitachi, Japan) to determine the morphology and elemental composition of the synthesized powders. Particle size analyses of the as-synthesized powders were carried out using a ZETA-potential and particle size analyzer (ELS-6000, Otsuka Electronics). Thermo-gravimetric analyses (TGA) were performed to evaluate the carbon deposition rate in the anodes. At first, the SLT-GDC composite powders were placed in a clean alumina crucible and they were then reduced at 800 °C for 6 h under flowing CH_4 at a flow rate of 100 cm^3 min^{-1}. The reduced powders were then analyzed by TGA (TA Q600, TA instruments, USA) under a constant air flow rate in the temperature range of 30 °C–1000 °C at a heating rate of 10 °C min^{-1}. Electrical conductivity was measured by means of a four-probe DC method in the temperature range of 400 °C–800 °C in H_2 or CH_4. The samples for the conductivity measurement were sintered at 1400 °C for 5 h in an air atmosphere.

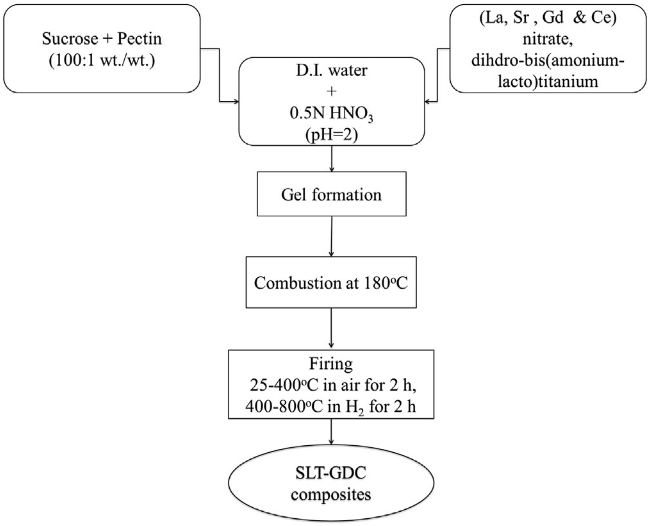

Fig. 1. Flow chart for the synthesis of the SLT-GDC composite powders using a modified sol–gel combustion technique.

Table 1
The compositions and the abbreviations of the synthesized SLT-GDC composite anode materials.

Anode material	Content of GDC (vol.%)
SLT	0
SLT-GDC12	12
SLT-GDC22	22
SLT-GDC30	30
SLT-GDC35	35
SLT-GDC40	40

2.3. Symmetric half-cell fabrication and electrochemical performance test

Symmetric half-cells with $La_{0.8}Sr_{0.2}Ga_{0.8}Mg_{0.2}O_{3-\delta}$ (LSGM) electrolyte were fabricated for electrochemical characterization. Commercial LSGM powder (LSGM, Fuel Cell Materials, USA) was compressed by cold iso-static pressing (CIP) and was then sintered at 1450 °C for 5 h to fabricate a 0.4-mm-thick LSGM electrolyte pellet. Anode paste was produced by mixing the anode powder and a binder (Heraeus V006) at a ratio of 70:30 wt.%. The paste was screen-printed on both sides of the LSGM pellet to make electrodes with a geometric area of 0.49 cm^2. Both electrodes were then fired at 1250 °C for 2 h. Pt mesh and Pt wire were used as the current collector and the lead, respectively. AC-impedance analysis was performed using a universal potentiostat with a frequency response analyzer (SP150, Biologic SAS, France) in a three-electrode configuration under humidified H_2 or CH_4 in the temperature range of 600 °C–800 °C. The applied frequency was in the range of 0.1 mHz–1 MHz with a voltage amplitude of 10 mV.

3. Results and discussion

3.1. Phase and morphology

The XRD patterns of all SLT-GDC composite anodes along with pure SLT are shown in Fig. 2. The peaks corresponding to both SLT and GDC patterns were detected without any trace impurity phases. There was a direct correspondence between peak height and the composition of the composite (e.g. the higher the GDC peak, the higher the GDC content of the composite). Variations in the mean crystallite sizes of SLT and GDC in SLT-GDC composite powder, which were calculated using the Scherrer equation, are plotted in Fig. 3. It is clear that the SLT-GDC35 composite has the lowest mean crystallite size compared to the other composites. The incorporation of GDC into the SLT matrix may suppress the grain growth of the SLT. The morphology of the as-synthesized powders before any further heat treatment is given in Fig. 4. As shown, the powders were highly crystalline and slightly agglomerated. The mean